From RVB to Skyrmion crystals: the many facets of spin Berry phases

Benoît Douçot
Dima Kovrizhin, Roderich Moessner, Nilotpal Chakraborty

December 6, 2023

LPTHE
LABORATOIRE DE PHYSIQUE
THEORIQUE ET HAUTES ENERGIES

cnrs
advancing the frontiers

SORBONNE
UNIVERSITÉ
CRÉATEURS DE FUTURS
DEPUIS 1257

Plan

- Spin Berry Phases in RVB early days
- Spin Berry phases in Quantum Hall ferromagnets

M. Berry (1984)

$$H = \mathbf{n}.\mathbf{S} \quad \mathbf{n}.\mathbf{n} = 1$$

$\mathbf{n} \in S^2$ is a parameter.

$$H|\Psi_\pm(\mathbf{n})\rangle = \mp|\Psi_\pm(\mathbf{n})\rangle$$

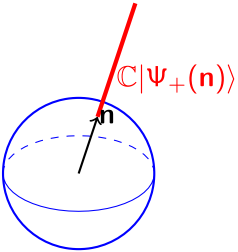

There exists no non-singular determination of $|\Psi_\pm(\mathbf{n})\rangle$ on the whole S^2 sphere : example of a non-trivial (complex) line bundle over S^2. The fibre over $\mathbf{n}$ is the (complex) line $\mathbb{C}|\Psi_\pm(\mathbf{n})\rangle$.

Note that projectors $P_\pm = |\Psi_\pm(\mathbf{n})\rangle\langle\Psi_\pm(\mathbf{n})|$ are smooth everywhere on S^2.

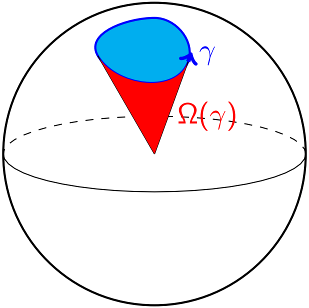

Berry connection

$$\boldsymbol{\mathcal{A}}_{\pm} = i\langle \Psi_{\pm}(\mathbf{n}) | \boldsymbol{\nabla} \Psi_{\pm}(\mathbf{n}) \rangle$$

$$\oint_{\gamma} \boldsymbol{\mathcal{A}}_{\pm}.d\mathbf{n} = \mp \Omega(\gamma) S$$

Berry curvature

$$\oint_{\gamma} \boldsymbol{\mathcal{A}}_{\pm}.d\mathbf{n} = \int_{\Omega} \boldsymbol{\mathcal{B}}_{\pm}.\mathbf{n} \quad \longrightarrow \quad \boldsymbol{\mathcal{B}}_{\pm} = \mp S \, \mathbf{n}$$

Chern number

$$\frac{1}{2\pi} \int_{S^2} \boldsymbol{\mathcal{B}}_{\pm}.\mathbf{n} = \mathcal{C}_{\pm} = \mp 2S \in \mathbb{Z}$$

Recollections from RVB early days (I)

PHYSICAL REVIEW B VOLUME 35, NUMBER 16 1 JUNE 1987

Topology of the resonating valence-bond state: Solitons and high-T_c superconductivity

Steven A. Kivelson,* Daniel S. Rokhsar,†,‡ and James P. Sethna†
Institute for Theoretical Physics, University of California, Santa Barbara, California 93106
(Received 9 March 1987; revised manuscript received 12 May 1987)

We study the topological order in the resonating valence-bond state. The elementary excitations have reversed charge-statistics relations: There are neutral spin-$\frac{1}{2}$ fermions and charge $\pm e$ spinless bosons, analogous to the solitons in polyacetylene. The charged excitations are very light, and form a degenerate Bose gas even at high temperatures. We discuss this model in the context of the recently discovered oxide superconductors.

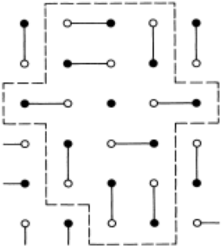

FIG. 2. The existence of a topological defect (here, a black soliton) can be deduced from a large loop enclosing it.

Hamiltonian involves modulation of nearest-neighbor hopping by lattice deformations.

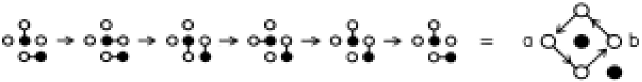

Recollections from RVB early days (II)

Gauge theory of high-temperature superconductors and strongly correlated Fermi systems

G. Baskaran and P. W. Anderson
Joseph Henry Laboratories, Department of Physics, Jadwin Hall, Princeton University, P.O. Box 708, Princeton, New Jersey 08544
(Received 6 July 1987)

In this paper we show that the development of resonating-valence-bond correlations and the subsequent superconducting order in the high-T_c oxide superconductors are described by an U(1) lattice-gauge theory. The insulating state has an almost-local gauge symmetry and doping changes this to a global symmetry, which is spontaneously broken at low temperatures, resulting in superconductivity. New topological excitations associated with the singlet field are found.

We believe that the nontopological unstable energetically stable point defects of the Δ field are likely to be the candidates for the spin solitons and charged solitons of KRS.[8] The following limiting case illustrates this. Imagine a dangling (unpaired) spin at the origin in an otherwise RVB vacuum. In this state clearly $\Delta_{0j}=0$, where j are the nearest neighbors of the site at the origin. If we take our mean-field Hamiltonian [Eq. (6)] and put $\Delta_{0j}=0$, the fermion degree of freedom at the origin is decoupled from the rest of the system and its energy is zero. We may identify this with the "midgap state." If this state is occupied we have a neutral soliton and have a charged soliton (hole) if this state is empty. The above situation is to be contrasted with the topological solitons in polyacetylene. The nontopological nature of the spin and charged soliton in our picture may be related to the possible *absence of any discrete symmetry breaking in the RVB state.*

Effective magnetic fields generated by spin textures (I)

Example: Motion of a hole in a static, twisted spin background

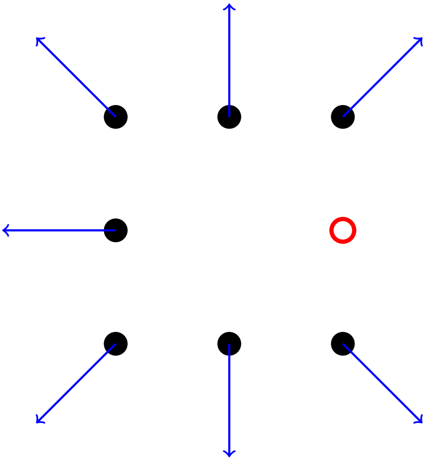

Effective magnetic fields generated by spin textures (I)

Example: Motion of a hole in a static, twisted spin background

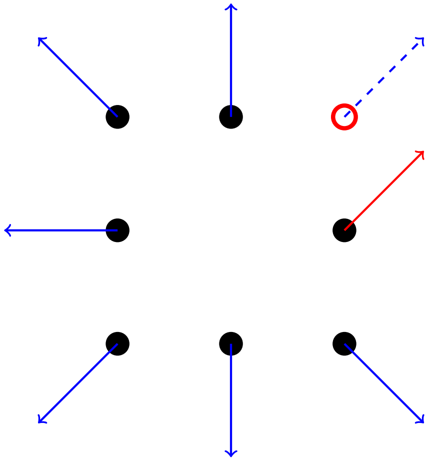

Effective magnetic fields generated by spin textures (I)

Example: Motion of a hole in a static, twisted spin background

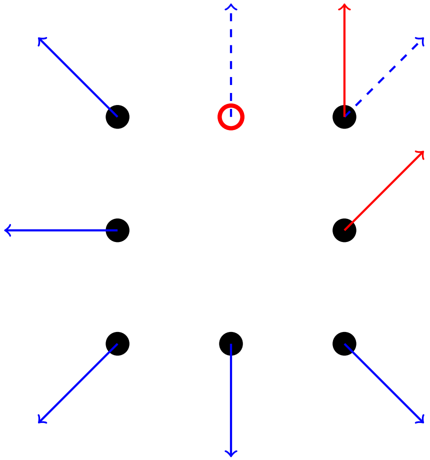

Effective magnetic fields generated by spin textures (I)

Example: Motion of a hole in a static, twisted spin background

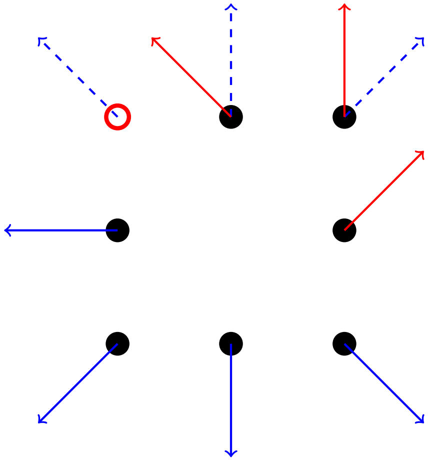

Effective magnetic fields generated by spin textures (I)

Example: Motion of a hole in a static, twisted spin background

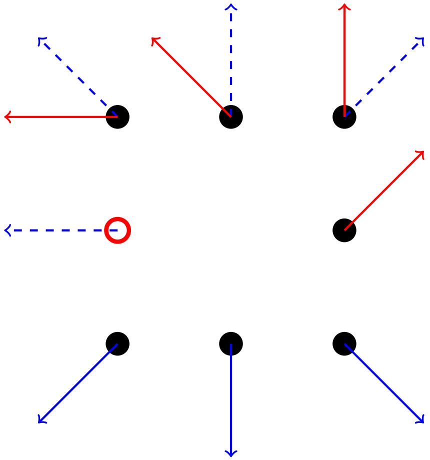

Effective magnetic fields generated by spin textures (I)

Example: Motion of a hole in a static, twisted spin background

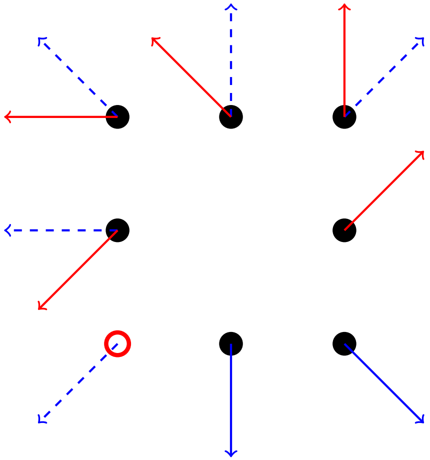

Effective magnetic fields generated by spin textures (I)

Example: Motion of a hole in a static, twisted spin background

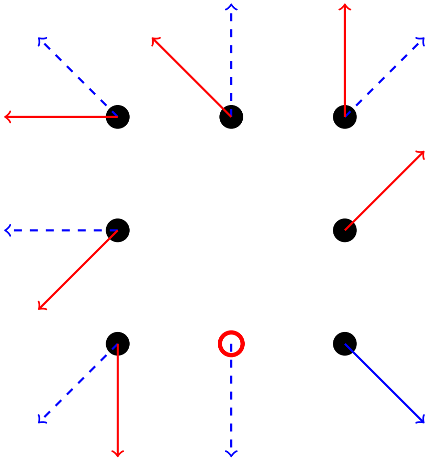

Effective magnetic fields generated by spin textures (I)

Example: Motion of a hole in a static, twisted spin background

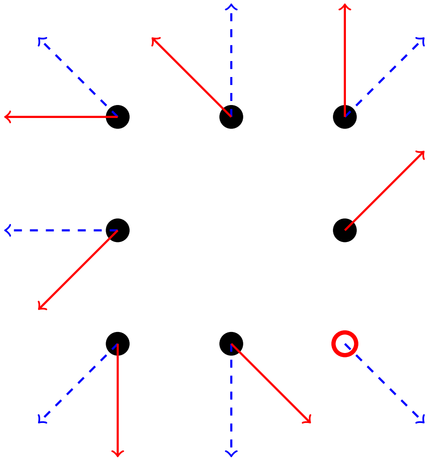

Effective magnetic fields generated by spin textures (I)

Example: Motion of a hole in a static, twisted spin background

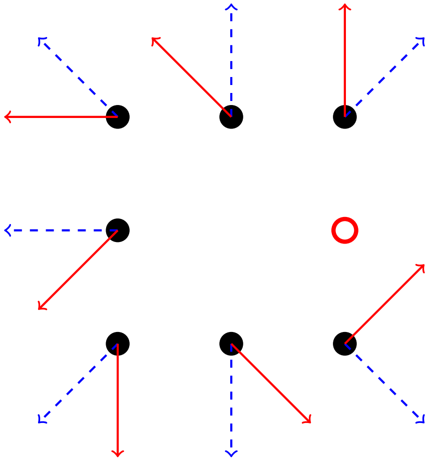

Effective magnetic fields generated by spin textures (II)

$$\begin{aligned} \text{Initial spin wave function: } |\mathrm{in}\rangle &= |\chi_1\rangle \otimes |\chi_2\rangle \otimes \cdots \otimes |\chi_{N-1}\rangle \otimes |\chi_N\rangle \\ \text{Final spin wave function: } |\mathrm{out}\rangle &= |\chi_2\rangle \otimes |\chi_3\rangle \otimes \cdots \otimes |\chi_N\rangle \otimes |\chi_1\rangle \end{aligned}$$

$$\langle \mathrm{out}|in\rangle = \langle\chi_2|\chi_1\rangle\langle\chi_3|\chi_2\rangle\cdots\langle\chi_N|\chi_{N-1}\rangle\langle\chi_1|\chi_N\rangle$$

In the limit of a smooth spin background:

$$\langle \mathrm{out}|in\rangle \to e^{i\oint_\gamma \boldsymbol{\mathcal{A}}_+ . d\mathbf{n}} = e^{-i\Omega(\gamma)S}$$

Applications

- Destruction of Nagaoka ferromagnetism in the $U = \infty$ Hubbard model, induced by mobile holes (B. D. and Xiao-Gang Wen, PRB (1989))
- Stabilization of Skyrmion crystals in Kondo lattice models
- Generation of artificial gauge fields in cold atom systems

Spin Skyrmions

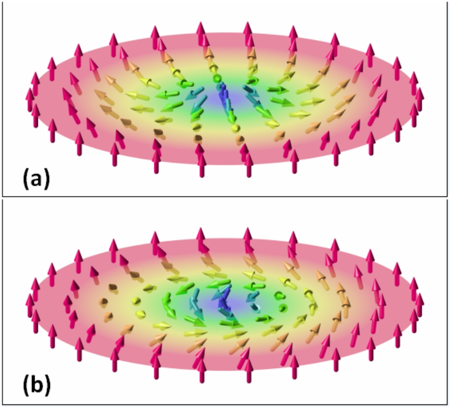

$$\pi_2(S^2) = \mathbb{Z}$$

(Picture from Wikipedia)

Skyrmion crystals in the $U = \infty$ Hubbard model ?

Assume static spin background, described by smooth unit vector field $\mathbf{n}_i$, with associated spin 1/2 wave functions $|\chi(\mathbf{n}_i)\rangle$.
Renormalized hopping amplitude: $t_{ij} = t\,\langle\chi(\mathbf{n}_i)|\chi(\mathbf{n}_j)\rangle$.

Phase of t_{ij} generates an effective magnetic field, with $\Phi/\Phi_0 = N_{\mathrm{Sk}}$.
Flux phases on a lattice: Fermi sea kinetic energy minimal when $N_{\mathrm{el}} = N_{\mathrm{Sk}}$, (Hasegawa et al. PRL 63, 907 (1989)). $\Delta_{\mathrm{phase}}E \sim -cx^3$, where x is the electron density.

Amplitude of t_{ij} is reduced by spin gradients:
$\langle|t_{ij}|\rangle \leq 1 - \frac{\pi}{2}N_{\mathrm{Sk}}/N_{\mathrm{sites}} = 1 - \frac{\pi}{2}x$, so $\Delta_{\mathrm{ampl}}E \sim +c'x^2$.

Skyrmion crystal has a lower energy when $x > x_* = c'/c$. For a square lattice, we found $x_* = 1/\pi$, (BD and R. Rammal, PRB 41, 9617 (1990)).

Plan

- Spin Berry Phases in RVB early days
- Spin Berry phases in Quantum Hall ferromagnets

Quantum Hall ferromagnets

N internal states (spin, valley, layer indices, e. g. $N = 4$ for graphene).
Integer filling factor M with $1 \leq M \leq N - 1$.
Large magnetic field $\rightarrow$ Projection onto the lowest Landau level (LLL). Assume that largest sub-leading term is given by Coulomb interactions (small g factor). This selects a ferromagnetic state

Main question: What happens when $\nu = M + \delta\nu$, $\delta\nu << 1$?

Quantum Hall ferromagnets

N internal states (spin, valley, layer indices, e. g. $N = 4$ for graphene).
Integer filling factor M with $1 \leq M \leq N - 1$.
Large magnetic field $\rightarrow$ Projection onto the lowest Landau level (LLL). Assume that largest sub-leading term is given by Coulomb interactions (small g factor). This selects a ferromagnetic state

Main question: What happens when $\nu = M + \delta\nu$, $\delta\nu << 1$?

Ferromagnetic state is replaced by slowly varying textures (e. g. Skyrmions lattices for $M = 1$): another striking manifestation of spin Berry phases.

Sondhi, Karlhede, Kivelson, Rezayi, PRB **47**, 16419, (1993), Brey, Fertig, Côté and MacDonald, PRL **75**, 2562 (1995)

Theoretical prediction: Brey, Fertig, Côté and MacDonald, PRL **75**, 2562 (1995)

Specific heat peak: Bayot et al. PRL **76**, 4584 (1996) and PRL **79**, 1718 (1997)

Increase in NMR relaxation: Gervais et al. PRL **94**, 196803 (2005)

Raman spectroscopy: Gallais et al, PRL **100**, 086806 (2008)

Microwave spectroscopy: Han Zhu et al. PRL **104**, 226801 (2010)

Example of entangled textures ($N = 4$, $M = 1$)

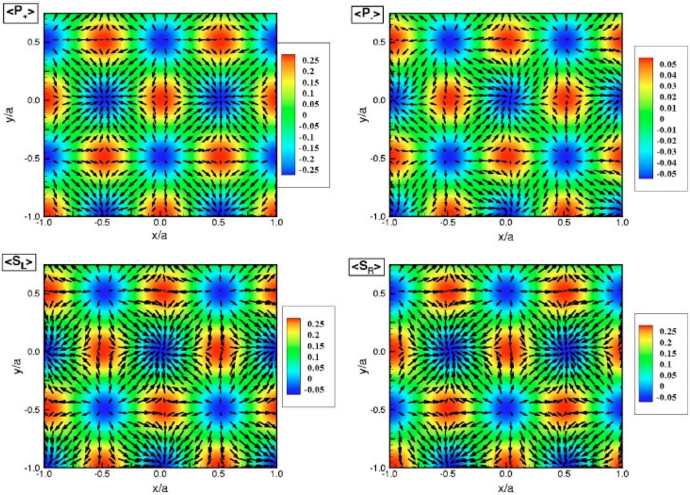

Bourassa et al, Phys. Rev. B **74**, 195320 (2006)

Optimal holomorphic maps from the torus to $\mathbb{C}\mathrm{P}(N-1)$

Choose a period lattice in the plane, generated by γ_1 and γ_2.
Theta functions are defined by: $\theta(z+\gamma) = e^{a_\gamma z + b_\gamma}\theta(z)$.
For a fixed type $\{a_\gamma, b_\gamma\}$, we get a fixed d, defined as the number of zeroes of θ functions in the (γ_1, γ_2) unit cell. This defines a d-dimensional space of θ functions (Riemann-Roch theorem).
Natural hermitian product: $(\theta, \theta')_d = \int d^2\mathbf{r}\ \exp(-\frac{\pi d|z|^2}{|\gamma_1 \wedge \gamma_2|})\overline{\theta(z)}\theta'(z)$
We pick an orthonormal basis: $(\theta_i, \theta_j)_d = \delta_{ij}$
Optimal textures ($d = N$) are obtained by choosing
$\psi_i(z) = \sum_j U_{ij}\,\theta_j(z)$ with $U \in \mathrm{SU}(N)$.
Spatial variations of topological charge: $Q(r)$ is always γ_1/d and γ_2/d periodic. At large d the modulation contains mostly the lowest harmonic, and its amplitude decays exponentially with d.
(D. Kovrizhin, BD, R. Moessner, PRL 110, 186802 (2013))

Recent experiments (2020)

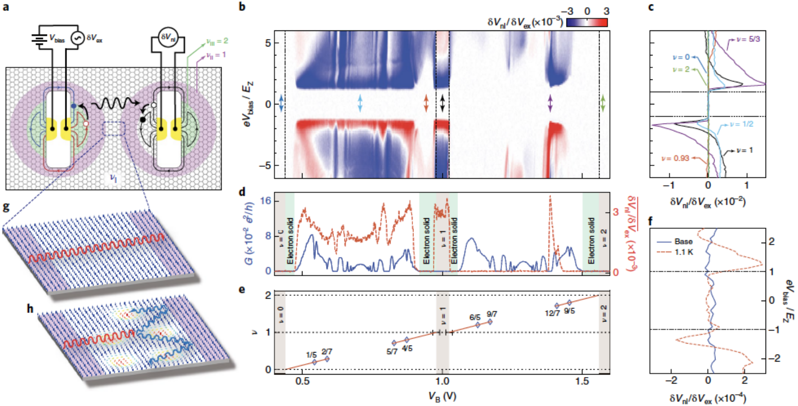

Magnon Landau levels induced by a Skyrmion (I)

Triangulation on the sphere (642 sites) (BD, D. Kovrizhin, R. Moessner, Annals of physics 399, 239 (2018))

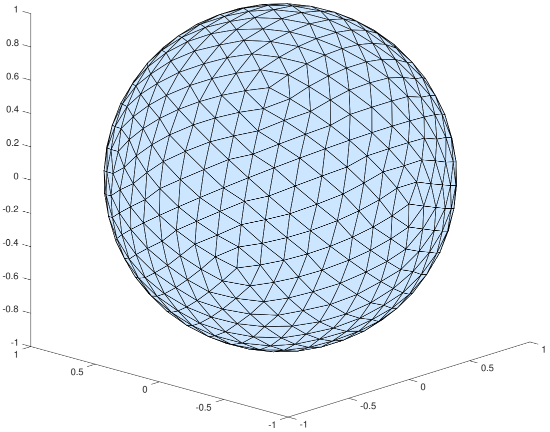

Magnon Landau levels induced by a Skyrmion (II)

Harmonic mode spectrum around a single Skyrmion classical configuration: compatible with the magnetic Laplacian on the sphere with a charge 2 magnetic monopole: manifestation of the spin Berry phase associated to a slow twist of the spin background.

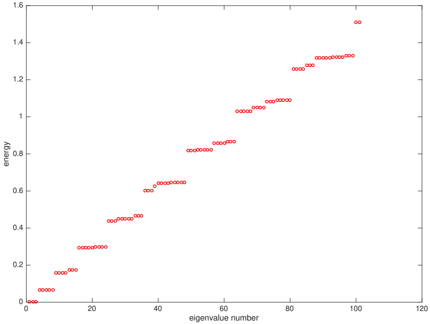

Neutron scattering experiments on MnSi

T. Weber et al., Science 375, 1025 (2022)

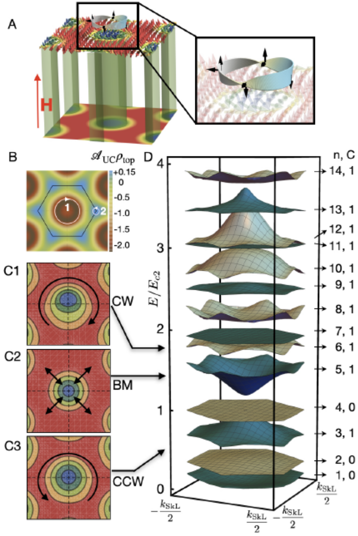

Modeling magnon scattering across a Skyrmion crystal

CHAKRABORTY, MOESSNER, AND DOUCOT PHYSICAL REVIEW B **108**, 104401 (2023)

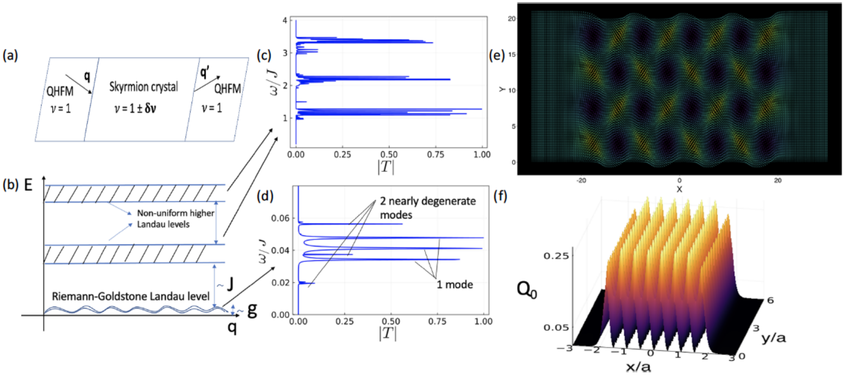

Holomorphic ansatz for slab geometry

Truncated θ functions:

$$\theta_p^{\mathrm{L}}(z) = \sum_{\nu \in \frac{p}{d}+\mathbb{Z} \text{ and } |\nu|<L} f_\nu(z) + c_{p,\mathrm{L}} f_{-N}(z) + c_{p,\mathrm{R}} f_N(z)$$

where $f_\nu(z) = \exp\left(-\pi d \nu^2 + 2\pi d \nu z/a\right)$.

$$\begin{aligned} \theta_p^{\mathrm{M}}(z) &\underset{x \to -\infty}{\simeq} c_{p,\mathrm{L}} f_{-N}(z) \\ \theta_p^{\mathrm{M}}(z) &\underset{x \to +\infty}{\simeq} c_{p,\mathrm{R}} f_N(z) \end{aligned}$$

Optimal textures ($d = N$) are obtained by choosing $\psi_i(z) = \sum_j U_{ij}\, \theta_j(z)$, where $U \in \mathrm{SU}(N)$ defines the desired Skyrmion crystal in the central region. $c_{p,\mathrm{L}}$ and $c_{p,\mathrm{R}}$ are then adjusted to match desired ferromagnetic states in left and right regions.

Perspectives: to include relevant anisotropies

For a graphene layer, one may consider:
$$E_A = \frac{\Delta_Z}{2}(u_p(M_{Px}^2 + M_{Py}^2) + u_z M_{Pz}^2 - M_{Sz})$$

Single Skyrmion Phase diagram

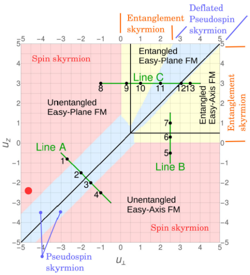

Lian and Goerbig, PRB 95, 245428 (2017)

Questions for a Skyrmion crystal

- Anisotropy energy » Coulomb energy → U matrix is non-invertible (rank 2).
- Coulomb energy » Anisotropy energy → U matrix is unitary.
- generalization to M filled Landau levels → Grassmannian textures. (BD, D. Kovrizhin, R. Moessner, arXiv:2107.10700)

Entanglement patterns with small anisotropies in $\mathbb{C}P^3$ crystals

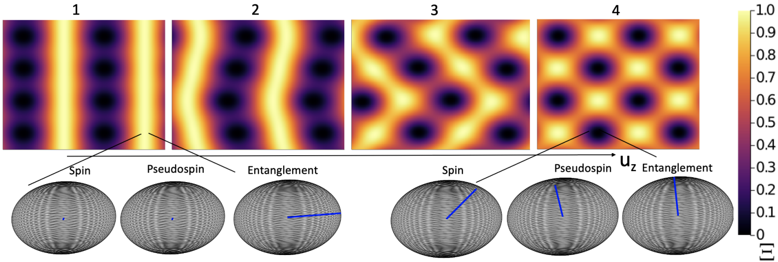

N. Chakraborty, BD, R. Moessner

Are Skyrmion crystals quantum mechanical objects?

Hybrid nature of Skyrmion crystals

- Stabilized by quantum effects (spin Berry phase, which creates effective magnetic fields).
- Spin Berry phase deeply affects magnon dynamics.
- Rich entanglement physics between spin and valley internal sectors.

Ubiquity of geometric quantization:

- Derivation of energy functionals and physical effects due to projection onto lowest Landau level.
- "Re-quantization" around classical textures and analysis of quantum zero point motion correction to total energy.
- More surprinsingly, provides a geometrical description of optimal textures, i.e. those with most uniform topological charge density.

Particle propagation across a uniform magnetic field strip

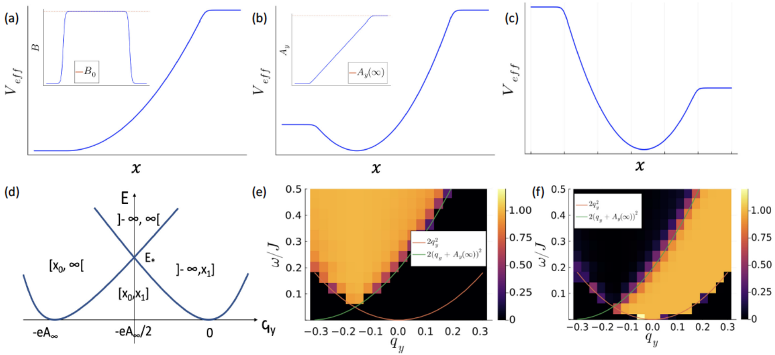

Case of a periodic modulation of B along y

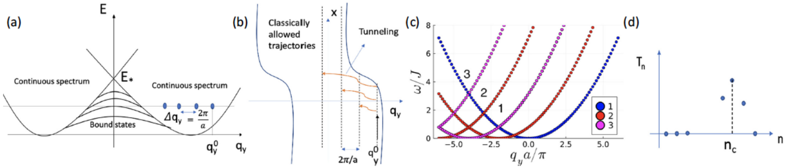

FIG. 3. Qualitative arguments for heuristic model with spatially modulated magnetic field along y axis. (a) Continuous spectrum for scattering and discrete spectrum for bound states. Modulation along transverse directions breaks q_y conservation and periodic modulation implies q_y is conserved modulo $2\pi/a$. Transmission below critical energy E_* is possible if the energy of one of the channels coincides with the bound state. (b) Pictorial description of the possibility of tunneling into other propagating channels due to crystalline order. Each channel has its effective potential profile and regions of allowed transmission as in Fig. 2(c)–2(f). The presence of multiple propagating modes allows transmission for an incoming magnon due to off-diagonal scattering. (c) Number of propagating modes in the $\omega - q_y$ plane in the unfolded zone scheme (for visual reasons). One can transfer this to the first Brillouin zone by standard folding techniques. Each color is for the two curves $2q_{yi}^2$ and $2(q_{yi} + A(\infty))^2$, such that in the region lying above both curves one gets an outgoing propagating mode for the ith channel, where $q_{yi} = q_y^{(0)} + 2\pi(i-1)/a$. For this figure we use $B_0 = 2\pi/a^2$ and $L = 20$. (d) Pictorial description of nonmonotonicity of channel resolved transmission from qualitative arguments presented in Sec. III B and figure (b) in this panel [not real data, see Fig 5(b)].

Particle propagation across a magnetic field strip

Case of a periodic modulation of B along y

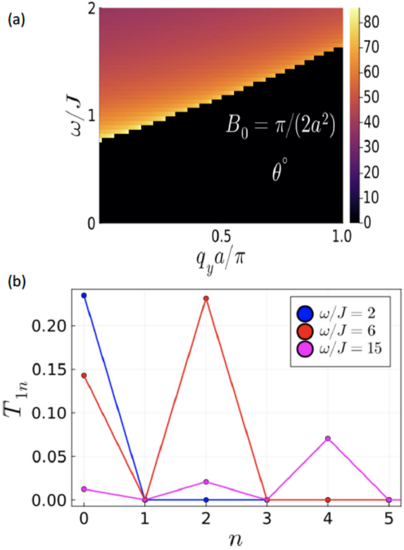

Holomorphic maps from the sphere to $\mathbb{CP}(N-1)$ (I)

$S^2 \cong \mathbb{CP}(1) \cong \mathbb{C} \cup \{\infty\}$ so we use one coordinate $z \in \mathbb{C}$.
Holomorphic maps $f : S^2 \to \mathbb{CP}(N-1)$: collections of N polynomials $P_1(z), \dots, P_N(z)$.
Topological charge: number of intersection points of $f(S^2)$ with an arbitrary hyperplane in $\mathbb{CP}(N-1)$ = maximal degree d of $P_1(z), \dots, P_N(z)$.
Topological charge density:

$$Q(z, \bar{z}) = (1 + |z|^2)^2 \partial_z \partial_{\bar{z}} \log(\sum_{i=1}^{N} |P_i(z)|^2)$$

$Q(z, \bar{z})$ is constant when:

$$\sum_{i=1}^{N} |P_i(z)|^2 = (1 + |z|^2)^d$$

Holomorphic maps from the sphere to $\mathbb{CP}(N-1)$ (II)

Hermitian scalar product on degree d polynomials:

$$(P,Q)_d = \frac{d+1}{\pi}\int d^2\mathbf{r}\ \frac{\overline{P(z)}Q(z)}{(1+|z|^2)^{d+2}}$$

Orthonormal basis: $e_p(z) = \begin{pmatrix} d \\ p \end{pmatrix}^{1/2} z^p$

General texture of degree d: $P_i(z) = \sum_{i=0}^{d} A_{ij} e_j(z)$

$Q(z,\bar{z})$ is constant when: $A^\dagger A = I_{d+1}$

If $d \geq N$: No solution

If $d \leq N-2$: many solutions, but not all components of the maps are linearly independent.

If $d = N-1$: $AA^\dagger = I_N = A^\dagger A$, so $(P_i, P_j)_d = \delta_{ij}$.

Textures with uniform topological charge density $\Leftrightarrow$ Components form an orthonormal basis.

Holomorphic maps from the sphere to $\mathbb{CP}(N-1)$ (III)

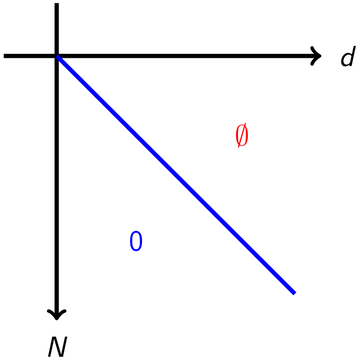

- 0 There exists a unique solution, up to global $SU(N)$ transformations, giving a uniform topological charge density
- $\emptyset$ No uniform solution exists: a kind of "fuzzy" charge crystal.

Holomorphic maps from Σ to $\mathbb{C}\mathrm{P}(N-1)$ (I)

Components of a map $f : \Sigma \to \mathbb{C}\mathrm{P}(N-1)$ were polynomials on the sphere and θ functions on the torus. Note that polynomials have poles at $z \to \infty$, and θ functions are multivalued.

More general construction: Pick a line bundle L over Σ, and choose the components of the maps $s_j(z)$ as global holomorphic sections of L, for $1 \leq j \leq N$.

Recipe for optimal textures: $N =$ dimension of the space of global holomorphic sections of L. Choose components forming an orthonormal basis for a well chosen hermitian product.

Holomorphic maps from Σ to $\mathbb{C}\mathrm{P}(N-1)$ (II)

Geometric quantization recipe for the hermitian product

ω : volume form associated to constant curvature metric on Σ

h^d : hermitian metric on fibers of L^d whose curvature form equals $-d(2\pi i)\omega$

$$(s, s')_{L,d} = \int_\Sigma h^d(s(x), s'(x))\omega(x)$$

Topological charge form: $\omega_{\rm top} - \omega = \frac{1}{\pi}\partial_z\partial_{\bar{z}} \log B(z, \bar{z})$.

$B(z, \bar{z})_{L,d} = \sum_{j=1}^N h^d(s_j(z), s_j(z))$

For an orthonormal basis $B(z, \bar{z})$ is the Bergman kernel, whose large d asymptotics has been studied a lot in the 90's.

Holomorphic maps from Σ to $\mathbb{CP}(N-1)$ (III)

Bergman kernel asymptotics (Tian, Yau, Zelditch, Catlin, Lu,...(1990 to 2000)):
$B(z,\bar{z}) = d + a_0(z,\bar{z}) + a_{-1}(z,\bar{z})d^{-1} + a_{-2}(z,\bar{z})d^{-2} + \dots$, such that $a_j(z,\bar{z})$ is a polynomial in the curvature and its covariant derivatives at $(z,\bar{z})$.

Interesting consequence: If ω is associated to the constant curvature metric on Σ, the previous family of textures have uniform topological charge, up to corrections which are smaller than any power of $1/d$.

"Practical" questions: How to effectively construct such orthonormal bases of sections, when Σ has genus ≥ 2 ?
Optimization of the exponentially small corrections in d with respect to the line bundle L ?

Maps $\Sigma \to \mathrm{Gr}(M, N)$ and rank M vector bundles (I)

Basic fact: there exists a 1 to 1 correspondence between:

- Maps $f : \Sigma \to \mathrm{Gr}(M, N)$
- Rank M vector bundles $\mathcal{V}$ over Σ, together with a choice of N sections of $\mathcal{V}$, which generate the fiber $\mathcal{V}_x$ at each $x \in \Sigma$, modulo automorphisms of $\mathcal{V}$.

$$\begin{array}{ccc} \mathcal{V} \cong f^*\mathcal{T}^* & \xrightarrow{\bar{f}} & \mathcal{T}^* \\ s_i \uparrow & 1 \leq i \leq N & \uparrow t_i \\ \Sigma & \xrightarrow{f} & \mathrm{Gr}(M, N) \end{array}$$

$\mathcal{T}^*$: dual of tautological rank M vector bundle over $\mathrm{Gr}(M, N)$. For $V \in \mathrm{Gr}(M, N)$, $t_i(V)$ is the linear form on V defined by the i-th component in $\mathbb{C}^N$ ($V \subset \mathbb{C}^N$).

Maps $\Sigma \to \mathrm{Gr}(M, N)$ and rank M vector bundles (II)

We start from a rank M vector bundle $\mathcal{V}$ over Σ, and a choice of N sections $s_i(x)$, $1 \leq i \leq N$ of $\mathcal{V}$, which generate the fiber $\mathcal{V}_x$ at each $x \in \Sigma$.

Using local frames in open subsets U_α covering Σ, each section $s_i(x)$ may be seen as an M-component row-vector. These N rows form an $N \times M$ matrix $V^{(\alpha)}(x)$, and if $x \in U_\alpha \cap U_\beta$:

$$V^{(\alpha)}(x) = V^{(\beta)}(x) t^{(\beta\alpha)}(x)$$

where $t^{(\beta\alpha)}(x)$ are the transition functions of $\mathcal{V}$.

The linear span in $\mathbb{C}^N$ of the columns of $V^{(\alpha)}(x)$ forms a well defined $f(x) \in \mathrm{Gr}(M, N)$.

Elements of $\mathcal{V}_x \longleftrightarrow M$-component row-vectors

Elements of $f(x) \longleftrightarrow N$-component column-vectors

$$\mathcal{V}_x \cong f(x)^*$$

Using the Plücker embedding of $\mathrm{Gr}(M, N)$ into $\mathbb{C}P(\tilde{N}-1)$

$$
\begin{array}{ccccc}
\mathrm{Det}\ \mathcal{V} & \xrightarrow{\overline{f}} & \mathrm{Det}\ \mathcal{T}^* & \xrightarrow{\overline{i_{\mathcal{P}}}} & \mathcal{O}(1) \\
\uparrow {\scriptstyle s_{i_1} \wedge \ldots \wedge s_{i_M}} & & \uparrow {\scriptstyle t_{i_1} \wedge \ldots \wedge t_{i_M}} & & \uparrow {\scriptstyle x_{i_1,\ldots,i_M}} \\
\Sigma & \xrightarrow{f} & \mathrm{Gr}(M, N) & \xrightarrow{i_{\mathcal{P}}} & \mathbb{C}P(\tilde{N}-1)
\end{array}
$$

$\tilde{N} = N!/(M!(N-M)!)$. Suggests to consider $i_{\mathcal{P}}\, f$, which is generated by the $\tilde{N}$ sections $s_{i_1} \wedge \ldots \wedge s_{i_M}$ of Det $\mathcal{V}$.

Main difficulty: An optimal texture $\Sigma \to \mathbb{C}P(\tilde{N}-1)$ is not always of the form $i_{\mathcal{P}}\, f$!